Biophysical Chemistry 24 (1986) 259–275
Elsevier

BPC 01077

OPTICAL ABSORPTION SPECTRA OF DEOXY- AND OXYHEMOGLOBIN IN THE TEMPERATURE RANGE 300–20 K

RELATION WITH PROTEIN DYNAMICS

Lorenzo CORDONE, Antonio CUPANE, Maurizio LEONE and Eugenio VITRANO

Istituto di Fisica dell'Universita' and GNSM-CISM, 90123 Palermo, Italy

Received 6th December 1985
Revised manuscript received 14th March 1986
Accepted 2nd April 1986

Key words: Deoxyhemoglobin; Oxyhemoglobin; Protein dynamics; Optical absorption spectrum

We have studied the optical absorption spectra of human deoxy- and oxyhemoglobin in the temperature range 300–20 K and in the wavelength range 350–1350 nm. By lowering the temperature, a narrowing and a shift of all bands were observed together with a sizeable increase of the integrated intensities of the charge-transfer bands of deoxyhemoglobin. At all temperatures the spectra are in full agreement with the band assignment previously suggested in the literature and no new relevant bands have been detected for both deoxy- and oxyhemoglobin. Analysis of the first and second moment of the bands, within the framework of the harmonic Franck-Condon approximation, gave information on the dynamic properties of the heme in the heme pocket.

1. Introduction

In this paper we report the spectra of deoxy- and oxyhemoglobin in the wavelength range 350–1350 nm and temperature range 300–20 K.

Measurements have been performed using a home-made apparatus that allows locking of the temperature to well within 0.2 K. Suitable handling allowed us to obtain transparent samples throughout the temperature range investigated; indeed, no cracking of the samples occurred and no variations in the baseline were observed (see section 2). This enabled us to perform the kind of data analysis we report.

By lowering the temperature, a narrowing of all measured bands and a frequency shift (either red or blue according to the particular band) have been observed. In the case of deoxyhemoglobin, the integrated intensities have an overall (20–300 K) approx. 7% increase for the bands ascribed [1,2] to $\pi \rightarrow \pi^*$ or d $\rightarrow$ d transitions; this increase is fully compatible with the increase in concentration due to sample contraction. In contrast, for bands ascribed to charge-transfer transitions (iron to porphyrin or porphyrin to iron) a relevant increase of the integrated intensities has been observed. In the case of oxyhemoglobin, an overall small increase of approx. 14% has been observed for all the bands investigated.

The behaviour of the investigated bands is in agreement with previously reported data on the temperature-induced difference spectra of deoxy- and oxyhemoglobin in the range 5–35°C [3]. The spectra at all temperatures are in agreement with the spectral assignment previously reported in the literature [1,2,4] and no new relevant bands are observed; moreover, the temperature dependence of oxyhemoglobin spectra is compatible with the assumption that the electronic ground state of oxyhemoglobin is a nondegenerate singlet ($S = 0$) [5].

The increase of the integrated intensities de-

tected for charge-transfer bands in deoxyhemoglobin enabled us to conclude that the distance of the iron from the mean porphyrin plane is temperature dependent; moreover, analysis of the first and second moment of the absorption bands within the framework of the harmonic Franck-Condon approximation gave information on the dynamics of the heme in the heme pocket. A brief description of the model and of the relationships for this analysis is reported in section 3. We believe that, despite the simplicity of the model and theoretical treatment, the analysis presented systematizes a large amount of data in a clear and concise way and contributes to the understanding of the optical spectra and internal dynamics of hemoglobin.

2. Experimental

Measurements were carried out using a homemade optical dewar whereby the temperature was lowered by flushing with liquid nitrogen or helium. The temperature was lowered, starting from room temperature, at a rate of approx. 1 K/min. The temperature intervals between two adjacent points were never larger than 15 K. Spectra were registered at constant temperature after 10 min equilibration. During measurements the temperature was held constant to well within 0.2 K using an adapted version of the temperature control described in ref. 6. Samples in suitable metacrylate cuvettes (ultraviolet grade, Kartell) were placed into the dewar at room temperature. Down to 40 K the sample pressure was held constant at 1 atm using a buffer balloon filled with hydrogen; at 40 K the gas in the sample region was pumped out. Samples contained hemoglobin at the concentration suitable for each band investigated, 65% (v/v) glycerol and 0.1 M phosphate buffer ($KH_2PO_4 + K_2HPO_4$, pH 7, in H_2O at room temperature). Under these solvent conditions hemoglobin maintains its functional properties [7]. Glycerol was RP grade purchased from Carlo Erba or Merck. The above procedure enabled us to have homogeneous and transparent samples in the whole temperature range explored. The hemoglobin concentrations (in heme) used were: 5×10^{-3}, 6×10^{-5} and 6×10^{-6} M for oxyhemoglobin in the near-infrared, visible and Soret bands, respectively; $3 \times 10^{-3} \div 6 \times 10^{-4}$, 6×10^{-5} and 6×10^{-6} M for deoxyhemoglobin in the near-infrared, visible and Soret regions, respectively. The optical path was usually 1 cm; this was reduced to 0.4 cm in the case of the near-infrared spectrum of oxyhemoglobin to reduce solvent absorption.

Hemoglobin was prepared and stored as already described [8]. Samples were prepared as follows: hemoglobin from highly concentrated stocks (~ 15%, w/v) was diluted in suitable water-glycerol-buffer solutions in order to obtain the final hemoglobin concentration in 65% (v/v) glycerol and 0.1 M phosphate buffer; in the case of the oxyhemoglobin near-infrared band, the samples were prepared by dialyzing the stock against suitable solvent before dilution. Oxyhemoglobin samples were put into the dewar without further manipulation. In the case of deoxyhemoglobin, 10-ml aliquots of the above samples were put into a tonometer and thoroughly deoxygenated; the deoxygenation was followed spectrophotometrically. After complete deoxygenation small aliquots (5 μl, Soret; 50 μl, visible; 200 μl, infrared bands) of a 4% (w/v) sodium dithionite ($Na_2S_2O_4$, Merck) solution were added anaerobically to the deoxygenated sample in the tonometer; sodium dithionite solutions were prepared using previously deoxygenated buffer as previously described [9]. Samples were then transferred to the cuvettes and dewar using equipment whereby the sample was always kept under a nitrogen atmosphere; indeed, no spectral alterations due to oxygenation were detected after transferral.

The baseline as a function of temperature was followed by performing sets of measurements with identical samples where only hemoglobin was missing. No baseline variations were observed in the 400–800 nm region in the whole temperature range explored; baseline variations were instead observed in the 800–1350 nm region, due to water and glycerol absorption and in the high-frequency limit of the Soret band, due to dithionite absorption (in the baseline relative to deoxyhemoglobin). For all measurements the baselines were registered and subtracted from the measured hemoglobin spectra before analysis.

The reproducibility of the measurements was very good and the same data were obtained when going from either high to low or low to high temperatures. Measurements were performed using a Cary 118C ultraviolet-visible spectrophotometer for Soret and visible absorption bands. For oxyhemoglobin the broad near-infrared band in the range 650–1350 nm was followed on a Cary 17 spectrophotometer, changing the detector at 800 nm so that the spectral bandwidth was always less than 2 nm. For deoxyhemoglobin the bands at approx. 680 and approx. 760 nm were followed using a Cary 118C spectrophotometer whereas the band at approx. 910 nm was followed using a Cary 17 spectrophotometer. For these last experiments the different spectral regions were taken together, after having normalized the spectra to the same hemoglobin concentration, exploiting the overlapping spectral region (780–803 nm); the exact value of hemoglobin concentration was determined at the end of each temperature scan using the cyanomethemoglobin method [10]. Both spectrophotometers were equipped with a digital data acquisition system controlled by a Rockwell Aim 65 microcomputer. Spectra, digitalized at 0.5 nm intervals, were registered on magnetic tape for off-line computer analysis.

Eventual shifts in the monochromator of the Cary 118C spectrophotometer were checked by scanning the 486 nm emission line of the deuterium lamp. This was done several times during each measurement using the 'reverse mode'. In agreement with the findings of Philo et al. [11], the uncertainty was of the order of ± 0.2 nm, i.e., much smaller than the overall band shifts we observed. In view of this result and due to the fact that larger band shifts were observed in the case of near-infrared bands, no wavelength calibration check was performed for measurements done using the Cary 17 spectrophotometer.

The deconvolution of the optical absorption spectra ($\epsilon(\nu)$) in terms of Gaussian components ($G(\nu) = A \exp[-(\nu - \nu_0)^2/2\sigma^2]$) was performed on an HP-1000 computer using a linearized least-squares fitting algorithm. All fittings were extremely good, although a slight increase in the χ value was observed at low temperature. Here $\chi = (\Sigma_i[A_i(\text{observed}) - A_i(\text{calculated})]^2/[N - p])^{1/2}$ where N is the number of data points (typically 300) and p the number of optimization parameters. The experimental variance of each point was considered to be constant and equal to the spectrophotometric precision in each spectral region. According to the standard definitions, the zeroth (M_0), first (M_1) and second (M_2) moment of each band are calculated as follows:

$$M_0 = \int \epsilon(\nu)\, d\nu$$

$$M_1 = \int \nu\epsilon(\nu)\, d\nu / M_0 \qquad (1)$$

$$M_2 = \int \nu^2\epsilon(\nu)\, d\nu / M_0 - M_1^2$$

3. Theoretical background

As is well known optical electrons are coupled to the motion of nearby nuclei; this phenomenon, which has been well studied for colour centers in crystals (see, e.g., refs. 12–16), causes a narrowing and a shift of the absorption band when the temperature is lowered.

A useful conceptual aid to the understanding of electron-vibration interactions is the well known configurational-coordinate diagram. Let us consider an ion with two electronic states between which it is possible to induce optical transitions; the energies of the states will depend on the distance of this particular ion from its neighbours. Such distances can be described by suitable normal coordinates Q_j. Within the framework of the harmonic approximation, the energy for both the ground and excited state of the optical electron will be quadratic in the difference between the coordinate Q_j and its equilibrium position. In general, due to the interaction of the optical electron with the nearby nuclei, the potential energy curve relative to the excited state will have a different equilibrium position (linear coupling) and a different curvature (quadratic coupling) than the potential energy curve relative to the ground state; moreover, the electronic transitions are assumed to take place instantaneously with respect to the time scale of nuclear motion, so that the nuclei

can be considered at rest during the transitions (Franck-Condon approximation). This situation is pictorially represented in fig. 1 for a particular normal coordinate Q_j. Within the framework of these approximations it has been shown [12] that the first and second moment of the absorption bands can be expressed as:

$$M_1 = \Delta E/h + 2\pi^2/h \sum_j \Delta_j^2 \nu_j^2(\mathrm{u}) + 1/4 \sum_j \left[\nu_j^2(\mathrm{u}) - \nu_j^2(\mathrm{g})\right]/\nu_j(\mathrm{g}) \times \coth\left[h\nu_j(\mathrm{g})/2kT\right]$$

$$M_2 = 2\pi^2/h \sum_j \Delta_j^2 \nu_j^4(\mathrm{u})/\nu_j(\mathrm{g}) \coth\left[h\nu_j(\mathrm{g})/2kT\right] + 1/8 \sum_j \left[\nu_j^2(\mathrm{u}) - \nu_j^2(\mathrm{g})\right]^2/\nu_j^2(\mathrm{g}) \times \coth^2\left[h\nu_j(\mathrm{g})/2kT\right] \quad (2)$$

where the sums are extended over the entire set $\{j\}$ of normal coordinates. In eqs. 2, ΔE is the energy difference between the excited and ground state when the nuclei are at rest in their equilibrium position; Δ_j the displacement of nuclear equilibrium positions, relative to the j-th normal mode, following the electronic promotion and therefore a measure of the linear coupling; and $\nu_j(\mathrm{g})$ and $\nu_j(\mathrm{u})$ the frequencies of the j-th normal mode when the electron is in the ground and excited state, respectively. The above quantities are also pictorially represented in fig. 1. Moreover, in eqs. 2 k and h are Boltzmann's and Planck's constants, respectively. In the expression of M_2 the first term is related to Δ_j (displacement effect) while the second is related only to the quadratic coupling (frequency effect); only the frequency effect contributes to the dependence of M_1 on temperature. Three quite reasonable assumptions are usually made in the treatment of experimental data [12–16]: (i) $[\nu_j(\mathrm{u}) - \nu_j(\mathrm{g})]/\nu_j(\mathrm{g}) \ll 1$; this means that the frequency effect can be safely neglected in M_2 with respect to the displacement effect; (ii) the spread in ν_j values is so small that a single mean effective frequency (ν) can be used both for M_1 and M_2 in eqs. 2; (iii) the presence of eventual high-frequency modes not populated in

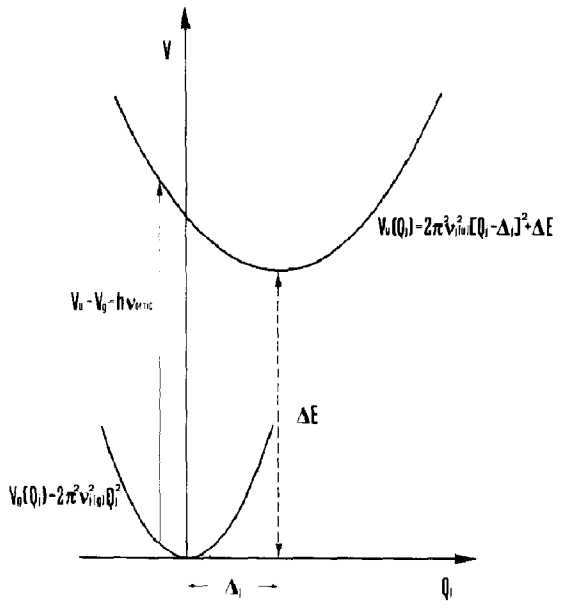

Fig. 1. Configurational coordinate diagram. $V_g(Q_j)$ and $V_u(Q_j)$ are the potential energy curves for the ground and excited electronic states, respectively.

the temperature range investigated contributes a constant and positive term C^2 to M_2 while the analogous contribution to M_1 can be included, together with the other constant terms already present, in the parameter D. Therefore, eqs. 2 reduce to:

$$M_1 = D + F \coth\left[h\nu/2kT\right]$$
$$M_2 = A \coth\left[h\nu/2kT\right] + C^2 \quad (3)$$

We consider it useful to point out that the parameter A is a measure of the electron-lattice linear coupling, i.e., of the lattice rearrangement following the electronic promotion, while the parameter F is a measure of the quadratic coupling, i.e., of the different shapes of the potential energy curves relative to the ground and excited electronic states. If the potential energy curve relative to the excited state is steeper than that relative to the ground state, a red shift of the absorption band will be observed by lowering the temperature ($F > 0$); in contrast, if the potential energy curve relative to

the excited state is smoother, a blue shift will be observed ($F < 0$).

4. Results and discussion

In the following we shall discuss, separately, the results concerning the different bands investigated.

4.1. Infrared bands (650–1350 nm)

Fig. 2 shows the near-infrared spectra of deoxy- (a) and oxyhemoglobin (b) at various temperatures. As can be seen, in the whole temperature range investigated, the deoxyhemoglobin spectra consist (as is more evident at low temperatures) of four main bands that have been ascribed [1,2] to an iron to porphyrin charge-transfer transition (band I), an iron d → d transition (band II) and two porphyrin to iron charge-transfer transitions (bands III and IV). A very small shoulder seems to appear at approx. 710 nm at low temperatures; in view of its weakness this shoulder is not considered in the forthcoming analysis. Oxyhemoglobin spectra consist, in the whole temperature range investigated, of a single broad band that has been mainly attributed [1,2] to the composition of two porphyrin to iron charge-transfer transitions (bands III and IV).

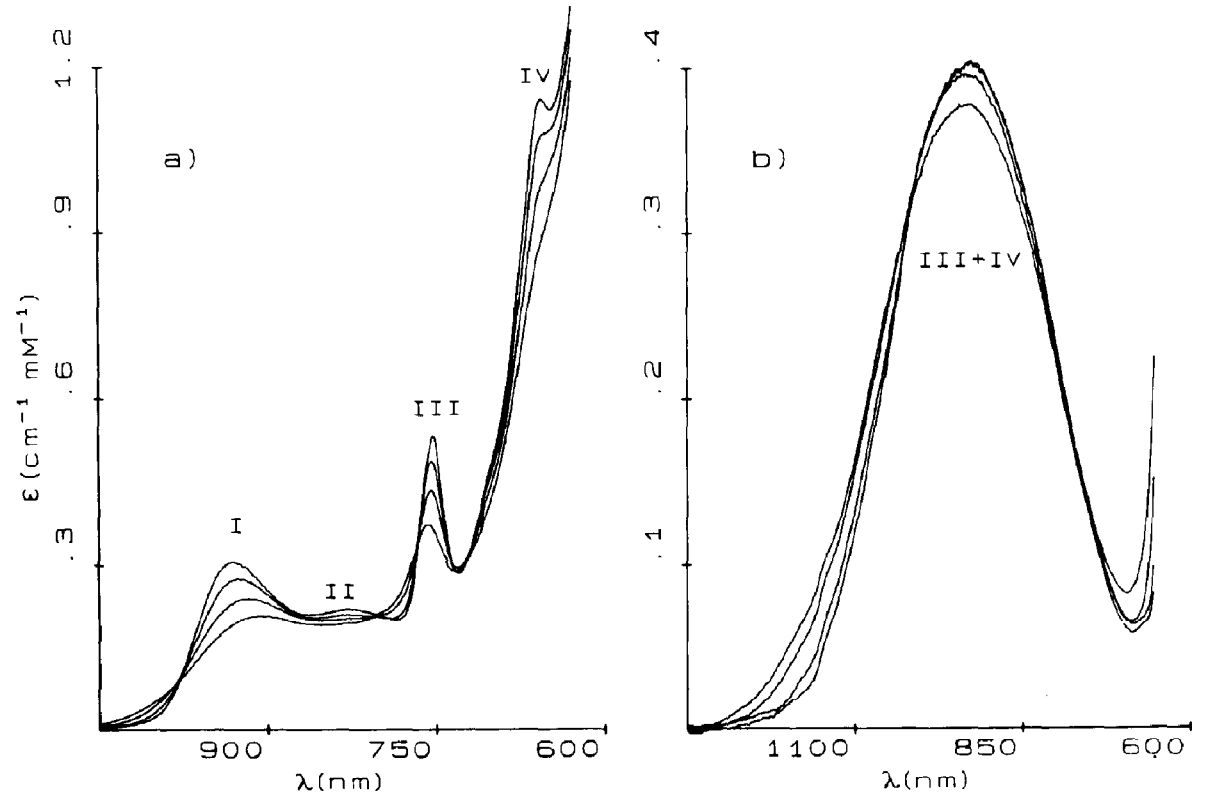

Fig. 2. Near-infrared absorption spectra (extinction coefficient on heme basis) of deoxy- and oxyhemoglobin at various temperatures. (a) Deoxyhemoglobin; from top to bottom (peak frequencies): $T = 20$, 120, 200, 298 K. (b) Oxyhemoglobin; from top to bottom (peak frequency): $T = 30$, 110, 215, 280 K. The bands are identified according to the notation in ref. 2.

The data in fig. 2a show a marked increase of the areas under bands I, III and IV, a red shift of band I, a blue shift of bands III and IV and a marked narrowing of all the bands on lowering of the temperature. Moreover, band II, not resolved at high temperature, becomes quite well resolved at low temperature.

The data in fig. 2b show that in the case of oxyhemoglobin a narrowing and blue shift of the absorption band take place on lowering the temperature, whereas the increase of the area under the curve is not as relevant as for bands I, III and IV of deoxyhemoglobin.

In order to obtain the zeroth, first and second moments of the measured bands for deoxyhemoglobin we successfully followed the deconvolution suggested in ref. 2; i.e., we considered the spectrum as arising from the above-mentioned four Gaussian bands plus a Gaussian extrapolation to fit the tail of higher frequency bands. Fig. 3a and b shows the fittings at high and low temperature, respectively. As shown, the fitting is extremely good at high temperature, while small misfits appear at low temperature; this can be due to the fact that at low temperatures the absorption bands are no longer strictly Gaussian [12].

In the case of oxyhemoglobin the attempts at resolving unambiguously in the whole temperature range the overall band in the terms suggested in ref. 2 were unsuccessful; therefore, in order to obtain the moments of the absorption band, we subtracted the tangent between the two minima of

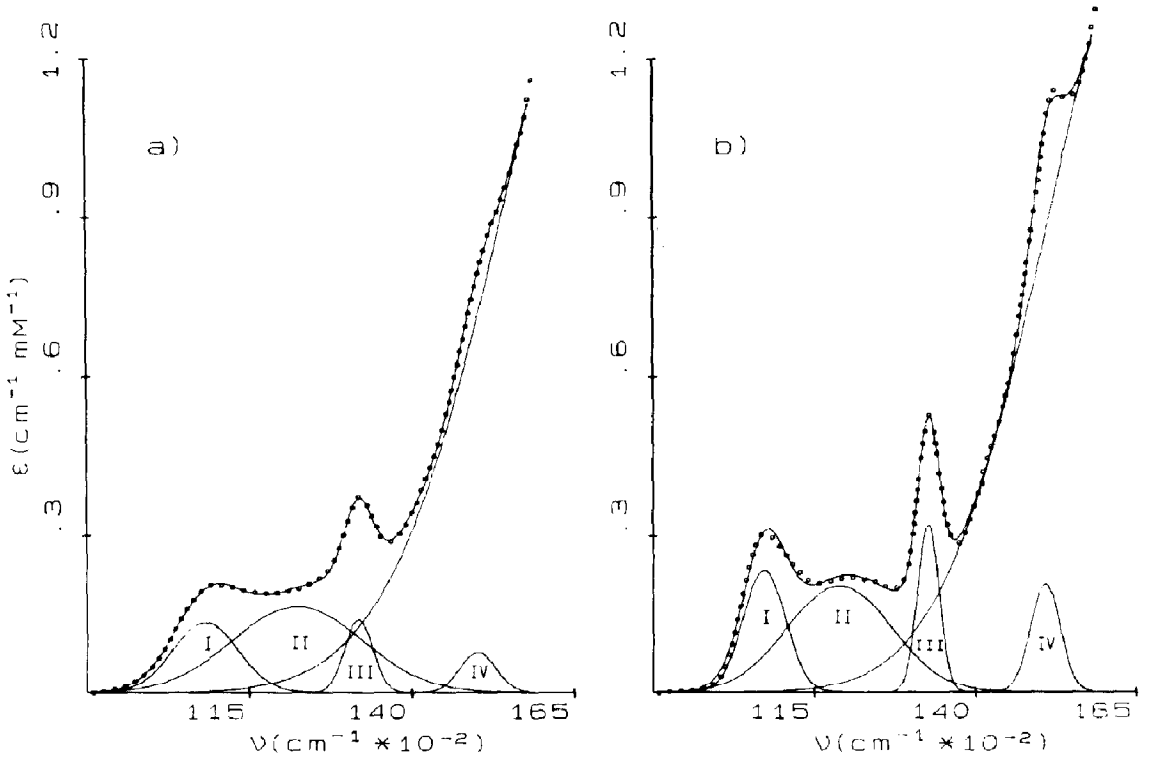

Fig. 3. Deconvolution of the near-infrared spectra of deoxyhemoglobin in terms of Gaussian components. (a) $T = 298$ K. (b) $T = 20$ K. Dots are the experimental points; the continuous lines represent the Gaussian components and the synthesized band profile. For the sake of clarity not all the experimental points have been reported. χ values (expressed in ϵ units) are 2.6×10^{-3} at $T = 298$ K and 7.5×10^{-3} at $T = 20$ K.

Table 1

Zeroth, first and second moment for near-infrared bands of deoxy- and oxyhemoglobin at 20 and 298 K

	M_0 (μ^{-1} cm^{-1} mM^{-1})		M_1 (μ^{-1})		M_2 (μ^{-2}) ($\times 10^3$)	
	$T = 20$ K	$T = 298$ K	$T = 20$ K	$T = 298$ K	$T = 20$ K	$T = 298$ K
Deoxyhemoglobin						
Band I	0.019	0.016	1.0722	1.0803	1.09	2.52
Band II	0.041	0.039	1.1876	1.2137	6.36	9.46
Band III	0.014	0.008	1.3260	1.3179	0.28	0.51
Band IV	0.012	0.005	1.5076	1.5023	0.53	0.78
Oxyhemoglobin						
Bands						
III + IV	0.12	0.11	1.1039	1.0865	13.5	14.7

Table 2

Values of the parameters obtained by fitting M_1 and M_2 of near-infrared bands in terms of eqs. 3

	A (μ^{-2}) ($\times 10^4$)	ν (cm^{-1})	C (μ^{-1}) ($\times 10^2$)	D (μ^{-1})	F (μ^{-1}) ($\times 10^2$)
Deoxyhemoglobin					
Band I					
$d_{xz} \rightarrow e_g(\pi^*)$	11.0	190	0	1.066	0.65
Band II					
$d_{xz} \rightarrow d_{z^2}$	25.0	200	6.2	1.166	2.10
Band III					
$a_{2u}(\pi) \rightarrow d_{yz}$	2.7	240	0	1.333	−0.76
Band IV					
$a_{1u}(\pi) \rightarrow d_{yz}$	5.3	350	0	1.518	−0.92
Oxyhemoglobin					
Band III, IV					
$a_{2u}(\pi) \rightarrow d_{xz} + O_2(\pi_g)$ $a_{1u}(\pi) \rightarrow d_{xz} + O_2(\pi_g)$	22.0	290	10.8	1.131	−2.80

the absorption curve at each temperature and calculated the moments of the resulting distributions using eqs. 1 and taking the two tangent points as integration limits.

In table 1 we report the values of the moments for the infrared bands of deoxy- and oxyhemoglobin at low and high temperatures. The values of M_0, M_1 and M_2 as a function of temperature are reported in figs. 4, 5a and 5b, respectively *. The continuous lines in fig. 5 repre-

* As can be seen from fig. 2a, at high temperature, band II of deoxyhemoglobin is quite unresolved. This brought about unreliable values of the parameters of Gaussian II at high temperature. Due to the large overlapping of Gaussians I and II this induced a nonmonotonic temperature dependence of M_0 of band I at high temperatures. To circumvent this inconvenience, we proceeded as follows. (i) We fitted the whole spectrum in terms of the above five Gaussian components with no constraints in the parameters in the temperature range 20–200 K. (ii) We fitted the M_1 and M_2 values obtained for band II in terms of eqs. 3. (iii) We imposed, in the fitting of the whole spectra at high temperatures, the M_1 and M_2 values of Gaussian II obtained from point (ii). By the use of this procedure, the high-temperature χ values for the whole spectra did not vary greatly with respect to those obtained in the fitting without constraints (e.g., $\chi = 2.6 \times 10^{-3}$ at $T = 298$ K, compared with $\chi = 2.5 \times 10^{-3}$ obtained, at the same temperature, in the fitting without constraints), while the parameters of Gaussian I (in particular M_0) showed much more regular behaviour.

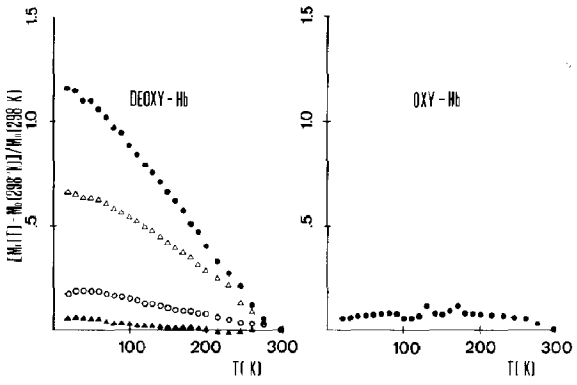

Fig. 4. Reduced M_0 values of the near-infrared bands as a function of temperature. Deoxyhemoglobin: (○) band I, (▲) band II, (△) band III, (●) band IV. Oxyhemoglobin; (●) bands III + IV.

sent the fitting of the M_1 and M_2 values according to eqs. 3. As is evident, the quality of the fitting is excellent except for M_1 of band IV of deoxyhemoglobin; this can be due to the fact that at high temperature this band is very poorly resolved and/or to the small shoulder appearing at approx. 710 nm at low temperature (see fig. 2a) having been neglected in the analysis. The values of the fitting parameters are reported in table 2. The data in figs. 4 and 5 and tables 1 and 2 confirm the conclusions previously drawn from inspection of the raw data. Although in the case of oxyhemoglobin bands III and IV were not resolved, we thought it reasonable to analyze M_1 and M_2 of the whole band in terms of eqs. 3. This was based on the results for deoxyhemoglobin which indicate (see table 2) that the electrons involved in the transitions relative to these bands probe, in their lower energy state, 'mean effective' frequencies of nuclear motion of the same order.

The sizeable increase of the integrated intensities (M_0) of bands I, III and IV of deoxyhemoglobin can be explained by considering that these bands arise from iron to porphyrin or porphyrin to iron charge-transfer transitions and therefore that their intensities are directly related to the overlapping between the iron d-orbitals and porphyrin π-orbitals involved in the transitions. The increase in M_0 observed by lowering the temperature indicates an increase of the above overlap and thus a variation of the relative distance (about 0.6 Å at room temperature [17,18]) between the iron atom and mean porphyrin plane. The fact that the above M_0 increase saturates at very low temperatures suggests that low-frequency anharmonic modes of the whole protein modulate the motion of the iron and are involved in this effect. The small M_0 increase of approx. 7% relative to band II is fully compatible with the increase of hemoglobin concentration due to thermal contraction and is in agreement with the attribution of this band to a $d \rightarrow d$ transition. In the case of oxyhemoglobin an approx. 10% overall increase in M_0 is observed. The smaller increase, as compared with deoxyhemoglobin charge-transfer bands, can be understood by considering that, in the case of oxyhemoglobin, the iron atom lies at the center of the porphyrin ring [17,18] and therefore that smaller overlap variations with temperature can be expected.

The data in table 2 indicate that: (i) electrons promoted from porphyrin to iron probe, in their lower energy state, a mean effective frequency of nuclear motion (ν) higher than that probed by electrons promoted from iron to porphyrin. This is confirmed by the fact that the iron to porphyrin charge-transfer band exhibits a red shift while the porphyrin to iron charge-transfer bands exhibit a blue shift on lowering of temperature; (ii) ν values for porphyrin to iron transitions are almost equal both for deoxy- and oxyhemoglobin. This indicates that the dynamic properties of the heme in the heme pocket, as probed by the electrons involved in these transitions, in their ground state, are not sizeably affected by the presence of the liganded oxygen. This does not contrast with the quite different quaternary conformations of oxy- and deoxyhemoglobin, since ν is the average frequency of modes localized in the heme that modulate the energy of electronic transitions; (iii) M_1 values relative to band II of deoxyhemoglobin red shift on lowering of the temperature (see also fig. 5a). According to the band assignment proposed in refs. 1 and 2, this would suggest that the mean effective frequency seen by the electron in the d_{z^2} orbital is higher than that in the d_{xz} orbital; (iv) no coupling with high-frequency nuclear motions is observed ($C^2 = 0$) for charge-

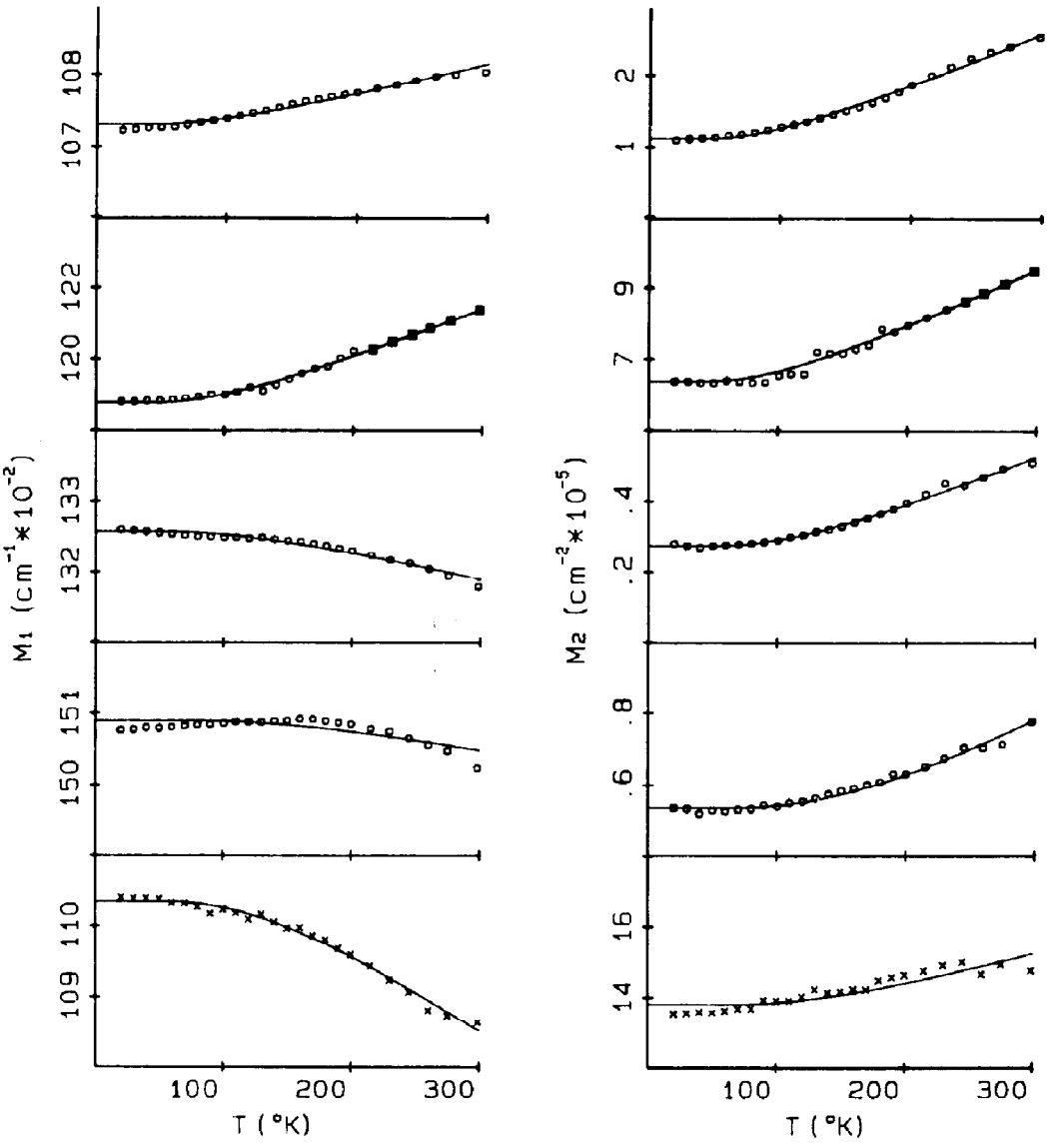

Fig. 5. M_1 and M_2 values of near-infrared bands as a function of temperature. (○) Deoxyhemoglobin, from top to bottom: band I, II, III, IV. (×) Oxyhemoglobin: bands III + IV. The continuous lines represent the fitting according to eqs. 3. (■) High-temperature values of M_1 and M_2 relative to band II, obtained following the procedure described in the footnote on p. 265.

transfer bands of deoxyhemoglobin. In this respect no conclusions can be drawn for charge-transfer bands of oxyhemoglobin, since bands III and IV are not resolved.

4.2. *Visible bands (500–650 nm)*

In fig. 6 we report the visible spectra of deoxy- (a) and oxyhemoglobin (b) at various tempera-

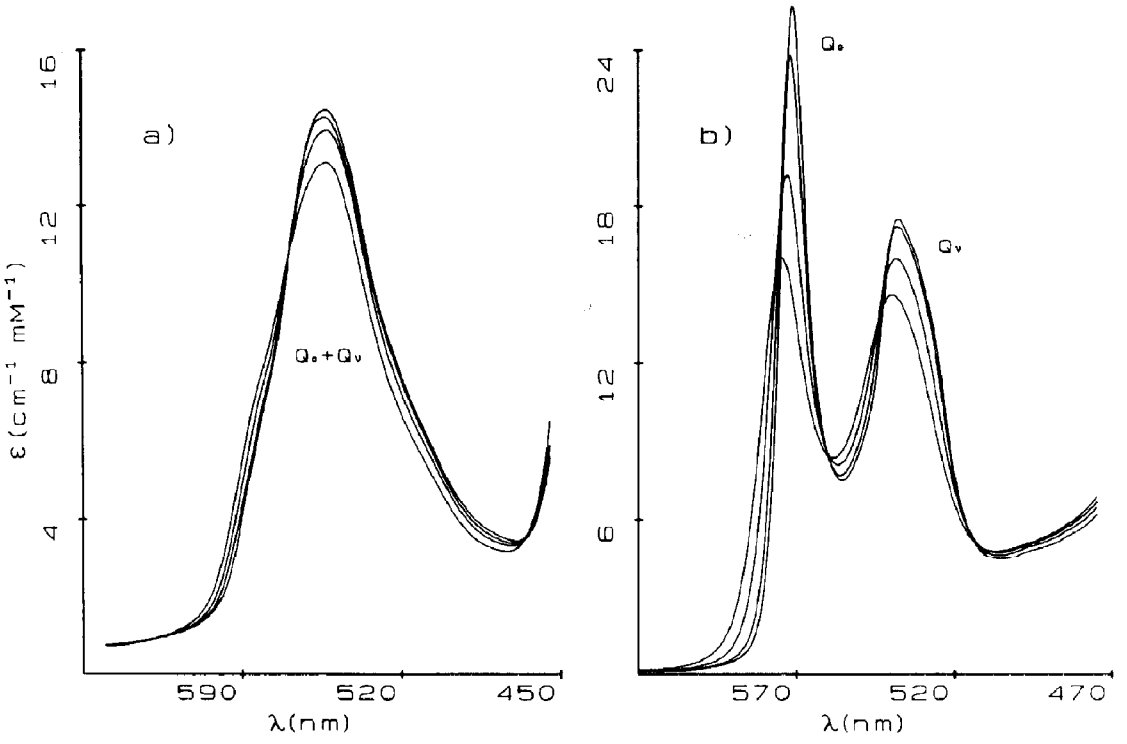

Fig. 6. Visible absorption spectra (extinction coefficient on heme basis) of deoxy- and oxyhemoglobin at various temperatures. (a) Deoxyhemoglobin; from top to bottom (peak frequency): $T = 15$, 110, 180, 298 K. (b) Oxyhemoglobin; from top to bottom (peak frequencies): $T = 27$, 100, 200, 280 K. The bands are identified according to the notation in ref. 2.

tures. As is shown, in the whole temperature range investigated the deoxyhemoglobin spectra consist of a single broad band; this has been attributed to a single porphyrin $\pi \rightarrow \pi^*$ electronic transition and arises from the overlapping of a fundamental absorption band (Q_0) with its vibronic one (Q_v) [1,2]; these bands are not well resolved even at very low temperatures. For oxyhemoglobin, the spectra consist of two main bands that have again been ascribed to a single porphyrin $\pi \rightarrow \pi^*$ transition, the high-frequency band Q_v being the vibronic of the low-frequency one Q_0 [1,2]; in this case the two bands are well resolved at all temperatures. In the case of deoxyhemoglobin the attempts at resolving unambiguously in the whole temperature range the overall band into the Q_0 and Q_v components were unsuccessful; therefore, as already done for the near-infrared band of oxyhemoglobin, we subtracted the tangent between the two minima of the absorption curve at each temperature and calculated the various moments of the resulting distributions. In the case of oxyhemoglobin we thought it reasonable to deconvolute the spectra in terms of four Gaussian components G_1, G_2, G_3 and G_4 and to calculate the moments of the distributions resulting from the sum $G_1 + G_2$ (Q_0) and from G_3 (Q_v). The Gaussian G_4 was necessary as an extrapolation, while Gaussian G_2 was necessary to obtain reasonable fittings. Fig. 7a and b shows the fitting at high and low temperature, respectively. As can be seen, the fitting is extremely good at high temperature, while small misfits appear at low temperature. It must be noted that the deconvolution of the Q_0 band into two Gaussians (G_1 and G_2) is a heuristic one and that no assignment to particular

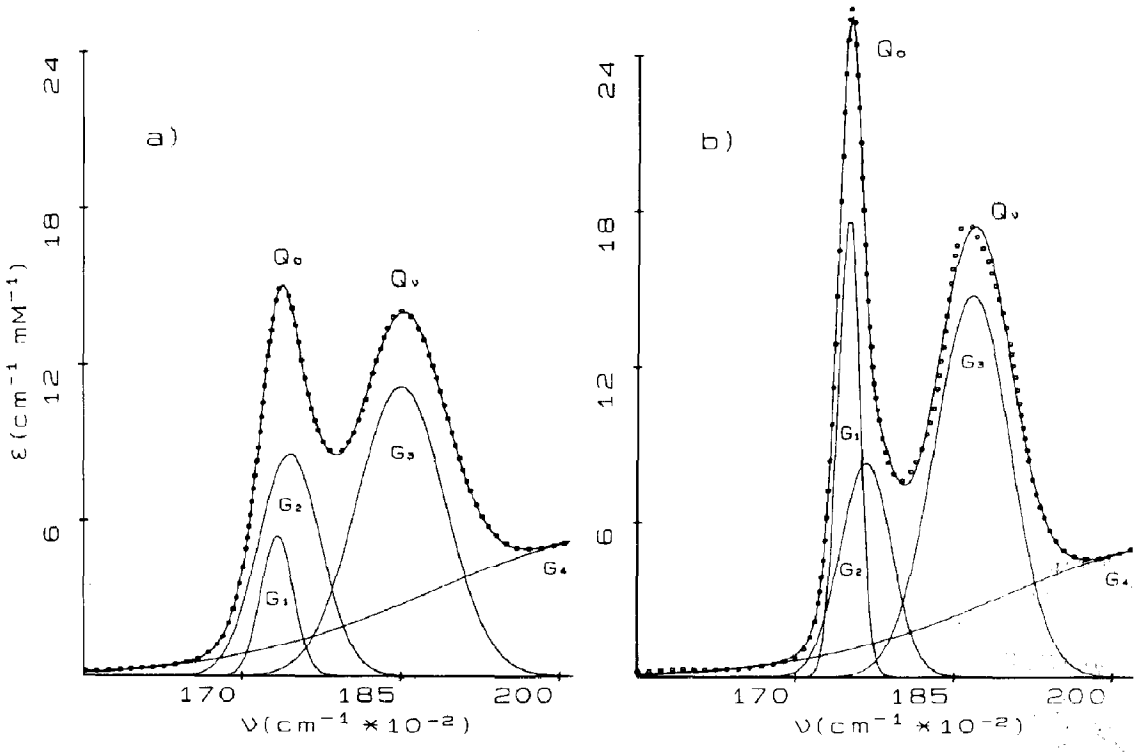

Fig. 7. Deconvolution of the visible spectra of oxyhemoglobin in terms of Gaussian components. (a) $T = 298$ K. (b) $T = 20$ K. Dots are the experimental points; the continuous lines represent the Gaussian components and the synthesized band profile. For the sake of clarity not all the experimental points have been reported. χ values (expressed in ϵ units) are 4×10^{-2} at $T = 298$ K and 2.5×10^{-1} at $T = 20$ K.

electronic transitions can be made for the two Gaussian components separately. However, we consider it worthy of mention that by lowering the temperature, both G_1 and G_2 exhibited monotonically half-width narrowing and blue shift of the peak frequencies.

In table 3 we report the values of the moments for the visible bands of deoxy- and oxyhemoglobin at low and high temperature. M_0, M_1 and M_2 values as a function of temperature are plotted in figs. 8, 9a and 9b, respectively. The continuous lines in fig. 9 represent the fittings of M_1 and M_2 according to eqs. 3. As shown, the quality of the fitting is excellent; the values of the fitting parameters are reported in table 4.

The small M_0 increase of approx. 7% relative to the visible band of deoxyhemoglobin is analogous to that previously reported in the case of band II; it can be ascribed to the increase in hemoglobin concentration due to thermal contraction and is in agreement with attribution of this band to a porphyrin $\pi \rightarrow \pi^*$ transition. In contrast, a slight, but meaningful, higher M_0 increase of approx. 14% is evident in the case of oxyhemoglobin for both Q_0 and Q_ν bands. If one considers that an approx. 7% increase can be ascribed to thermal contraction, then one should find that a further approx. 7% increase in the M_0 values is present. Following the orbital promotion mechanism suggested in refs. 1 and 2, one could explain this increase by considering that the ground state wave function of the electron undergoing the optical transition does not describe, in oxyhemoglobin, a pure porphyrin π state, but rather that it also

Table 3

Zeroth, first and second moment for visible and Soret bands of deoxy- and oxyhemoglobin at 20 and 298 K

	M_0 (μ^{-1} cm^{-1} mM^{-1})		M_1 (μ^{-1})		M_2 (μ^{-2}) ($\times 10^3$)	
	$T = 20$ K	$T = 298$ K	$T = 20$ K	$T = 298$ K	$T = 20$ K	$T = 298$ K
Deoxyhemoglobin bands $Q_0 + Q_\nu$	2.396	2.234	1.8368	1.8200	7.09	7.19
Oxyhemoglobin band Q_0	0.978	0.841	1.7580	1.7423	0.43	0.74
Oxyhemoglobin band Q_ν	1.333	1.166	1.8661	1.8500	1.30	1.73
Deoxyhemoglobin band B	25.86	24.52	2.3985	2.3915	7.60	8.70
Oxyhemoglobin band B	23.93	20.98	2.4379	2.4302	6.50	7.10

Table 4

Values of the parameters obtained by fitting M_1 and M_2 of visible and Soret bands in terms of eqs. 3

	A (μ^{-2}) ($\times 10^4$)	ν (cm^{-1})	C (μ^{-1}) ($\times 10^2$)	D (μ^{-1})	F (μ^{-1}) ($\times 10^2$)
Deoxyhemoglobin band $Q_0 + Q_\nu$					
$a_{1u}(\pi), a_{2u}(\pi) \rightarrow e_g(\pi^*)$	0.9	280	8.0	1.861	−2.5
Oxyhemoglobin band Q_0					
$a_{1u}(\pi), a_{2u}(\pi) \rightarrow e_g(\pi^*)$	3.9	270	0.7	1.777	−2.0
Oxyhemoglobin band Q_ν					
$a_{1u}(\pi), a_{2u}(\pi) \rightarrow e_g(\pi^*)$	6.3	290	2.6	1.889	−2.4
Deoxyhemoglobin band B					
$a_{1u}(\pi), a_{2u}(\pi) \rightarrow e_g(\pi^*)$	27.0	350	7.1	2.413	−1.4
Oxyhemoglobin band B					
$a_{1u}(\pi), a_{2u}(\pi) \rightarrow e_g(\pi^*)$	14.0	350	7.1	2.454	−1.6

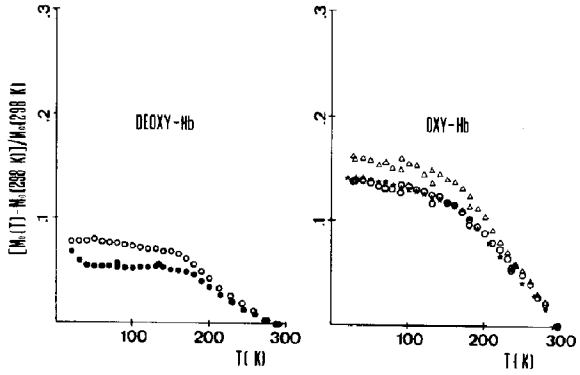

Fig. 8. Reduced M_0 values of the visible and Soret bands as a function of temperature. Deoxyhemoglobin: (○) band ($Q_0 + Q_\nu$), (●) band B. Oxyhemoglobin: (△) band Q_0, (○) band Q_ν, (★) band B.

contains contributions from iron d-orbitals. This is in agreement with the fact that, due to the presence of the ligand, the iron is brought into the heme plane. Due to anharmonicity, this orbital mixing could increase on lowering the temperature, bringing about the observed M_0 increase. This interpretation is in full agreement with the fact that CO-hemoglobin also shows a similar M_0 increase (this laboratory, unpublished results).

The data in table 4 indicate that: (i) the ν values are almost equal for the Q_0 and Q_ν bands of oxyhemoglobin; this was to be expected since these two bands originate from the same electronic transition; (ii) in analogy to the findings relative to porphyrin to iron charge-transfer bands, the ν values are almost the same for both oxy-

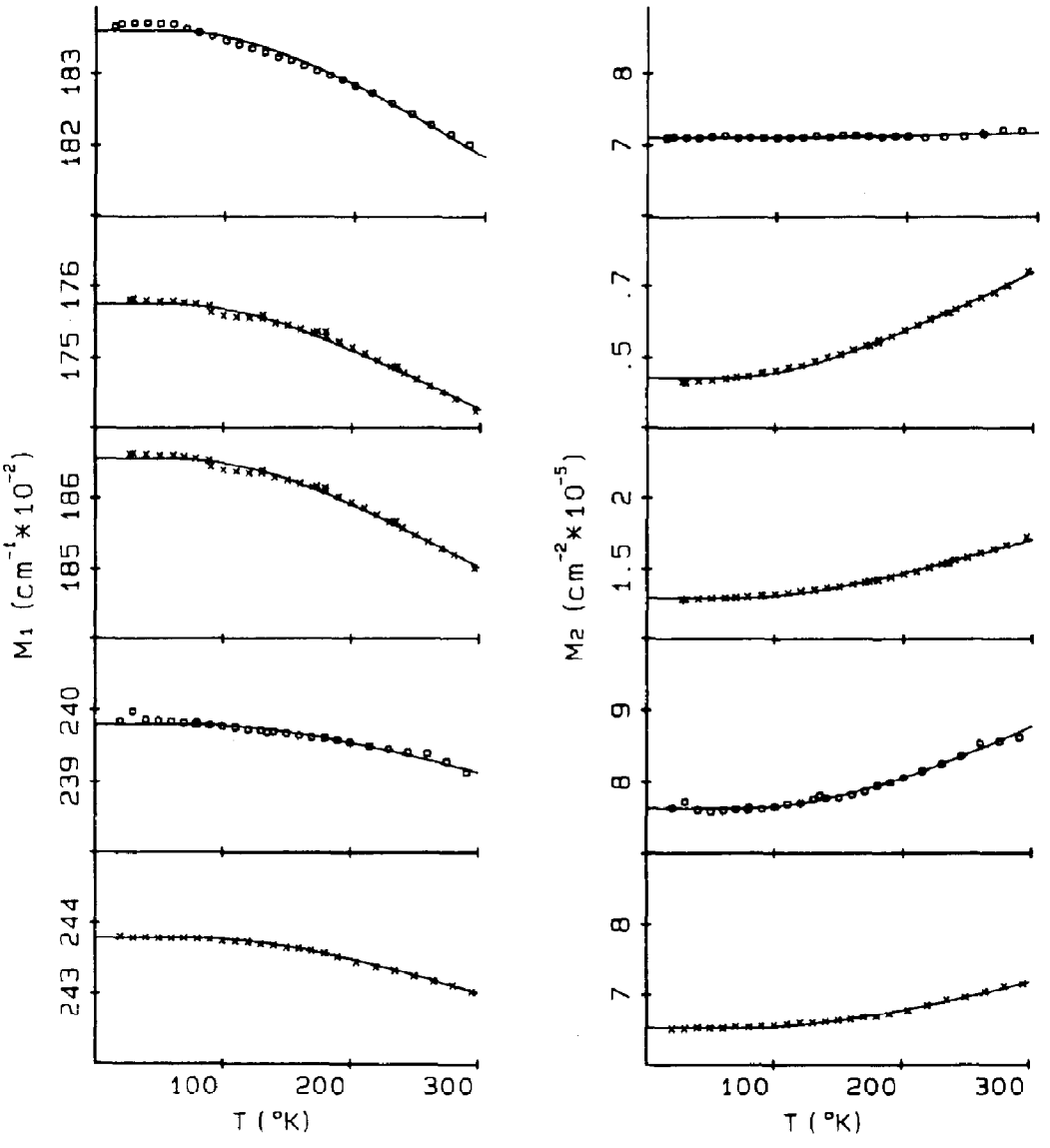

Fig. 9. M_1 and M_2 values of visible and Soret bands as a function of temperature. (○) Deoxyhemoglobin, from top to bottom: band $Q_0 + Q_\nu$, B. (×) Oxyhemoglobin; from top to bottom: band Q_0, Q_ν, B. The continuous lines represent the fitting according to eqs. 3.

and deoxyhemoglobin; (iii) the ν values obtained are almost the same as those for porphyrin to iron charge-transfer bands. Points (ii) and (iii) were fully expected on the basis of the configuration coordinate model, since the electronic promotions responsible for visible and for porphyrin to iron charge-transfer bands involve the same porphyrin ground state orbitals; (iv) sizeable and almost equal C^2 values are found in the M_2 fitting for Q_0 and Q_ν bands of oxyhemoglobin; as mentioned in

section 3, a nonvanishing C^2 value indicates a coupling with high-frequency modes whose frequencies lie outside the distribution that determines the ν values reported in table 4. This is consistent with the presence of the high-frequency modes that bring about the Q_ν vibronic absorption band; (v) to fit the M_2 values in the case of deoxyhemoglobin a very small A and a large C^2 value are needed; due to the fact that we did not succeed in resolving the Q_0 and Q_ν bands, we believe it is meaningless to draw conclusions from these findings. We stress however that, as already mentioned, the ν value obtained from the fitting of M_1 is in full agreement with the analogous values obtained for other transitions involving electronic promotions starting from porphyrin orbitals.

4.3. Soret bands (350–500 nm)

In fig. 10 we report the spectra of the Soret bands of deoxy- (a) and oxyhemoglobin (b) at various temperatures. As can be seen, in the whole temperature range investigated, the spectra consist, for both deoxy- and oxyhemoglobin, of a single band that has been attributed [1,2] to porphyrin $\pi \rightarrow \pi^*$ electronic transitions. The data in fig. 10 show a blue shift and a narrowing of the bands on lowering of temperature; moreover, a larger increase of the area under the curve is evident for oxyhemoglobin.

In order to obtain the zeroth, first and second moments of the measured bands in the case of deoxyhemoglobin we considered it reasonable to analyze only the contribution relevant to the band

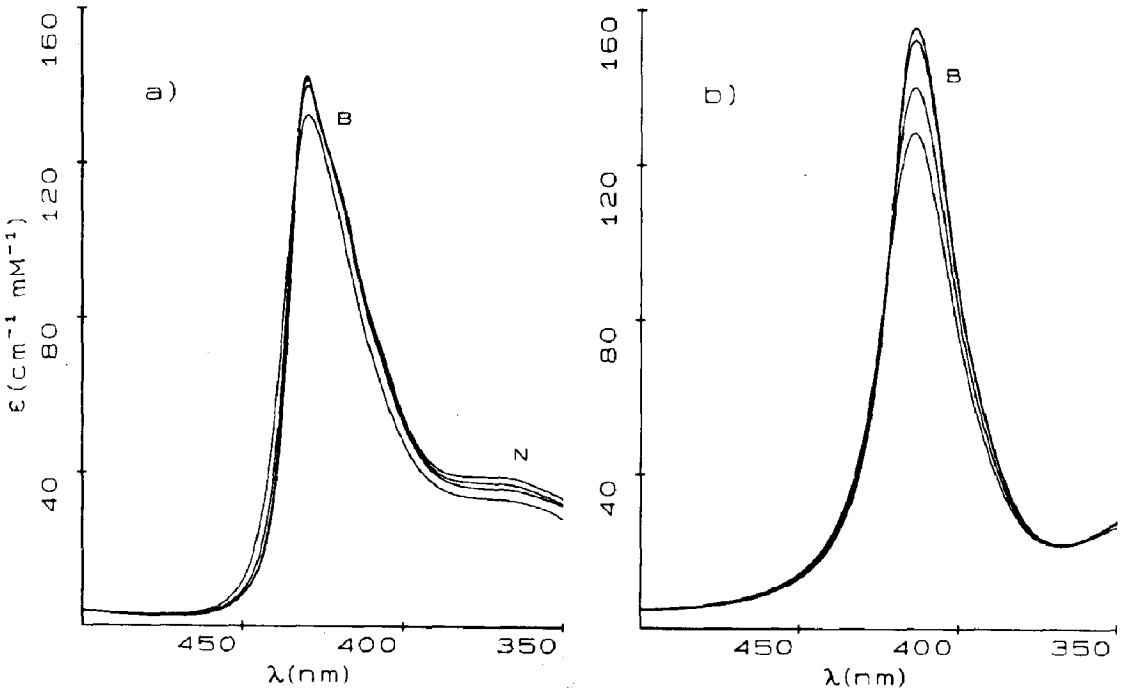

Fig. 10. Soret absorption spectra (extinction coefficient on heme basis) of deoxy- and oxyhemoglobin at various temperatures. (a) Deoxyhemoglobin; from top to bottom (peak frequency): $T = 20$, 100, 180, 298 K. (b) Oxyhemoglobin; from top to bottom (peak frequency): $T = 20$, 110, 220, 298 K. The bands are identified according to the notation in ref. 2.

(see fig. 11). For this purpose we deconvoluted the relevant part of the spectra in terms of three Gaussian components and calculated the moments of the distribution resulting from their sum. It must again be noted that our deconvolution is a heuristic one and that no assignment to particular electronic transitions can be made for each Gaussian component. The deconvolution is not dependent upon the truncation point at low wavelengths within 20 nm. By lowering the temperature, all Gaussian components exhibit monotonically half width narrowing and a blue shift of the peak frequencies.

In the case of oxyhemoglobin we subtracted the tangent between the two minima of the absorption curve at each temperature and calculated the moments of the resulting distributions.

In table 3 we report the values of the moments for the Soret bands of deoxy- and oxyhemoglobin at low and high temperatures. The values of M_0, M_1 and M_2 as a function of temperature are plotted in figs. 8, 9a and 9b, respectively. The values of the fitting parameters are reported in table 4. The data in figs. 8 and 9 and tables 3 and 4 confirm the conclusions previously drawn from inspection of the raw data.

The behaviour of M_0 for both deoxy- and oxyhemoglobin is identical to that of the visible bands, i.e., an approx. 7% increase in the case of deoxyhemoglobin and approx. 14% increase for oxyhemoglobin. An analogous 14% increase in M_0 is also found for the Soret band of CO-hemoglobin (unpublished results). This fact confirms the interpretation already presented in the discussion of visible bands.

The data in table 4 and fig. 9 indicate that for

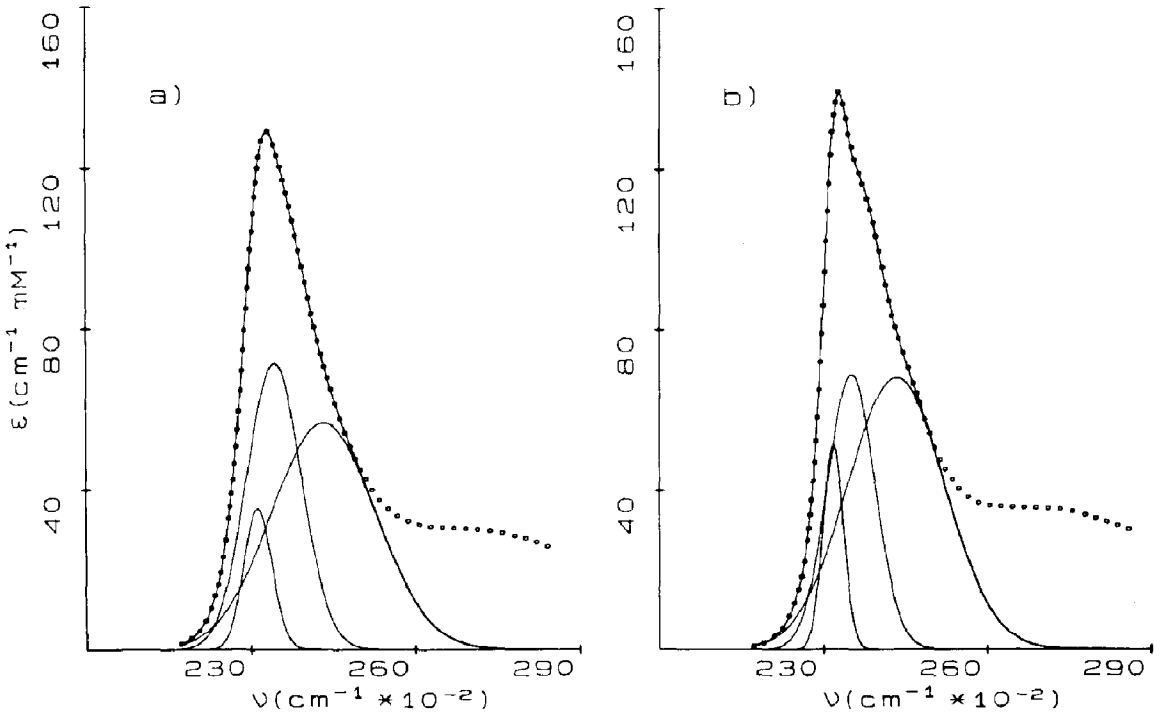

Fig. 11. Deconvolution of the B band (Soret region) of deoxyhemoglobin in terms of Gaussian components. (a) $T = 298$ K. (b) $T = 20$ K. Dots are the experimental points; the continuous lines represent the Gaussian components and the synthesized band profile. For the sake of clarity not all the experimental points have been reported. χ values (expressed in ϵ units) are 0.17 at $T = 298$ K and 0.32 at $T = 20$ K.

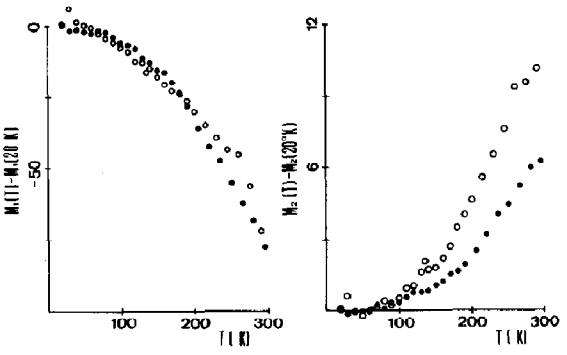

Fig. 12. M_1 and M_2 of the Soret bands (offset scale) as a function of temperature. (○) Deoxyhemoglobin; (●) oxyhemoglobin. M_1 scale is in cm^{-1}; M_2 scale in $\mu^{-2} \times 10^4$.

Soret bands, the ν values are also almost equal for deoxy- and oxyhemoglobin and nonzero C^2 values are obtained. This last fact is in agreement with the existence of vibronic absorptions of Soret bands. The data in table 4 in particular indicate that the ν and F values are almost equal for both deoxy- and oxyhemoglobin, whereas the A values are significantly different; this is evidenced in fig. 12 where M_1 and M_2 values are reported on an offset scale. From the definition of parameter A (see section 3) it follows that its value is a measure of the 'lattice' rearrangement following the electronic promotion, and therefore it is directly related to the coupling of the electron in the excited state with neighbouring nuclei. Since the excited state orbital $[e_g(\pi^*)]$ is more delocalized toward the porphyrin periphery than the ground state orbital $[a_{1u}(\pi), a_{2u}(\pi)]$, it follows that the larger A value in the case of deoxyhemoglobin is indicative of greater interaction of the electron with neighbouring nuclei.

5. Conclusions

From the reported data the following conclusions can be drawn:

(1) The temperature dependence of the observed spectra confirms the band assignment suggested by Eaton and co-workers [1,2]. In particular, the $d \rightarrow d$ band at approx. 820 nm, not resolved at room temperature, is clearly visible in the low-temperature spectra of deoxyhemoglobin.

(2) The temperature dependence of the absorption spectra of oxyhemoglobin does not indicate the presence of thermal spin equilibrium [19,20] of the kind reported by Browett and Stillman [21] for catalase-azide and catalase-isothiocyanate complexes. The optical spectra at all temperatures are compatible with the assumption that the electronic ground state of oxyhemoglobin is a nondegenerate singlet ($S = 0$) [5].

Moreover, from the analysis of the data within the framework of the harmonic Franck-Condon approximation, the following further conclusions can be drawn:

(3) A simple harmonic oscillator model is sufficient to rationalize the temperature behaviour of the first and second moments of the observed bands; second-order effects, due to anharmonicity, are evident only in the temperature dependence of the zeroth moment, where first-order effects are missing. These last effects indicate that the distance of the iron from the mean porphyrin plane in deoxyhemoglobin is temperature dependent. Such an effect could, in principle, be relevant in the regulation of the functional properties of hemoglobin by temperature.

(4) The values of the obtained mean effective frequencies of nuclear motions are of the order of 200–350 cm^{-1}, i.e., of the order of the iron-proximal hystidine stretching vibration frequency observed by resonance Raman spectroscopy (see ref. 22 and references quoted therein). Heme vibrations in the range 1300–1600 cm^{-1} [22] could be responsible for the vibronic bands in the visible and Soret regions and for the presence of non-zero C^2 terms in the fitting of the second moments of visible and Soret bands.

(5) The linear coupling between the porphyrin π^*-orbitals and the nearby nuclei is larger for deoxyhemoglobin than for oxyhemoglobin. This fact is in agreement with a more open shape of the distal side of the heme pocket in oxyhemoglobin than in deoxyhemoglobin, as observed by X-ray crystallography [17,23] (especially for β-chains).

Acknowledgements

We wish to thank Professors G. Baldini, R. Boscaino, M. Fontana, E. Mulazzi, M.U. Palma, M.B. Palma-Vittorelli, F.S. Persico and N. Terzi for useful discussions. The technical assistance of Mrs. S. Francofonte, V. Greco, G. Lapis, A. Mangano, S. Pappalardo and G. Riccobono is also gratefully acknowledged.

References

1 W.A. Eaton and J. Hofrichter, Methods Enzymol. 76 (1981) 175.
2 W.A. Eaton, L.K. Hanson, P.J. Stephens, J.C. Sutherland and J.B.R. Dunn, J. Am. Chem. Soc. 100 (1978) 4991.
3 P.L. San Biagio, E. Vitrano, A. Cupane, F. Madonia and M.U. Palma, Biochem. Biophys. Res. Commun. 77 (1977) 1158.
4 D.A. Case, B.H. Huynh and M. Karplus, J. Am. Chem. Soc. 101 (1979) 4433.
5 L. Pauling and C.D. Coryell, Proc. Natl. Acad. Sci. U.S.A. 22 (1936) 210.
6 P.M. Angelo, M.U. Palma and G. Valana, Rev. Sci. Instrum. 38 (1967) 415.
7 D. Bulone, A. Cupane and L. Cordone, Biopolymers 22 (1983) 119.
8 L. Cordone, A. Cupane, P.L. San Biagio and E. Vitrano, Biopolymers 18 (1979) 1975.
9 L. Cordone, A. Cupane and S.L. Fornili, Biopolymers 22 (1983) 1677.
10 D.L. Drabkin and J.M. Austin, J. Biol. Chem. 12 (1935) 51.
11 J.S. Philo, M.L. Adams and T.M. Schuster, J. Biol. Chem. 256 (1981) 7917.
12 J.J. Markham, Rev. Mod. Phys. 31 (1959) 956.
13 G. Baldini, E. Mulazzi and N. Terzi, Phys. Rev. 140 (1965) 2094.
14 Y. Farge and M.P. Fontana, Electronic and vibrational properties of point defects in ionic crystals (North-Holland, Amsterdam, 1979).
15 Y.E. Perlin, Soviet Phys.-Usp. 6 (1964) 542.
16 H.I.G. Meyer, Physica 21 (1955) 253.
17 M.F. Perutz, Nature 228 (1970) 726.
18 G. Fermi, M.F. Perutz, B. Shaanan and R. Fourme, J. Mol. Biol. 175 (1984) 159.
19 M. Cerdonio, S. Morante, D. Torresani, S. Vitale, A. De-Young and R.W. Noble, Proc. Natl. Acad. Sci. U.S.A. 82 (1985) 102.
20 J.P. Savicki, G. Lang and M. Ikeda-Saito, Proc. Natl. Acad. Sci. U.S.A. 81 (1984) 5417.
21 W.R. Browett and M.J. Stillman, Biophys. Chem. 19 (1984) 311.
22 S.A. Asher, Methods Enzymol. 76 (1981) 371.
23 B. Shaanan, J. Mol. Biol. 171 (1983) 31.